Chemistry and Electronics of the Ge(111) Surface

Thesis by

David Knapp

In Partial Fulfillment of the Requirements

for the Degree of

Doctor of Philosophy

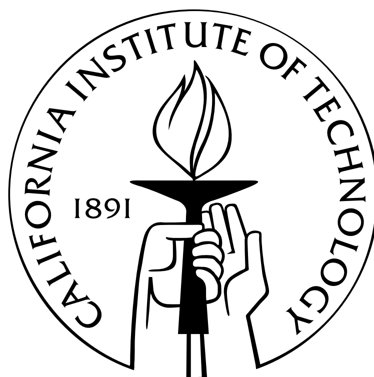

California Institute of Technology

Pasadena, California

2011

(Defended December 1, 2010)

© 2011

David Knapp

All Rights Reserved

Acknowledgements

Caltech has been an amazing place and I have many people to thank. I would first like to thank my advisor, Prof. Nathan Lewis, for his patience, advice, and for giving me the opportunity to work on interesting projects. I am also grateful to Dr. Bruce Brunschwig for his advice and assistance. I thank my committee members, Professors Jacqueline Barton, Mitchio Okumura, and Harry Atwater, who have been encouraging.

I need to extend my thanks to so many members of the Lewis Group, current and former, for their help in and out of the lab. Thanks to Lauren Webb, Joseph Nemanick, Florian Gstrein, and David Michalak for helping me get started, and for continued advice afterward. My thanks also to Patrick Hurley, Stephen Maldonado, and Erik Johansson, who were great postdocs to work with. Thanks to Brian Sisk and Elizabeth Mayo for the diversions outside the lab. Everyone in the Lewis Group has been kind and helpful; I am leaving off too many names.

Of course, I would not be here without the many years of help from my parents, Bruce Knapp and Ann Therrien.

Abstract

The halogenation/alkylation procedure that has been proven to chemically and electrically passivate the Si(111) surface has been adapted for application to Ge(111). Removal of the Ge(111) surface oxide with 6–9 M HF(aq), followed by exposure to Br_2 vapor, then alkylmagnesium or alkyllithium reagents yields air stable surfaces with surface recombination velocities (SRVs) as low as 40 cm/sec^{-1} at flat-band conditions. Surface charges with a density on the order of 10^{12} cm^{-2} cause a negative surface potential of almost 300 mV in n-type CH_3-Ge(111) samples prepared with this method. The oxidized surface shows a strongly positive surface potential in atmospheric conditions. A negative surface potential is also present in CH_3-Si(111), but the wider bandgap prevents this from causing inversion conditions in extrinsic samples. Ge(111) surfaces alkylated with a larger organic group, such as ethyl or decyl, displayed a weaker surface potential and higher surface recombination velocity as the surface was brought near flat-band. Mercury contacts to alkylated n-type substrates form rectifying junctions with barrier heights of 0.6 $\pm$ 0.1 eV. Contacts to p-type substrates or to oxidized n-type substrates show no measurable rectification. X-ray photoelectron spectroscopy (XPS) confirms that the area concentration of surface-bound carbon on CH_3-Ge(111) surfaces is equal to that of CH_3-Si(111)

surfaces. Other passivation methods were less successful.

Every atop Ge atom of an ideal CH_3-Ge(111) should be capped and the Ge-C bonds should be directed normal to the surface plane. Infrared absorption spectroscopy (IRAS) of methyl-terminated surfaces prepared from HF-etched precursors did not display distinguishable absorption peaks, but if the Ge substrate is first treated with an anisotropic etch before the HF etch, IRAS confirms the methyl group orientation with the polarization-dependent “umbrella” mode absorption at 1232 cm^{-1} and a polarization-independent rocking mode at 755 cm^{-1}. Well-ordered CH_3-Ge(111) surfaces displayed less surface charging while maintaining the low SRVs, indicating that such surfaces are successfully passivated.

Contents

Acknowledgements **iii**

Abstract **iv**

1 Introduction **1**

1.1 Background 1

1.1.1 Semiconductors 1

1.1.2 Surface Potential 2

1.2 Silicon & Germanium 5

1.2.1 Germanium 6

1.3 Summary 8

2 Chemical Passivation of Ge(111) Surfaces **12**

2.1 Background 12

2.1.1 X-Ray Photoelectron Spectroscopy 16

2.1.1.1 Elemental Analysis 16

2.1.1.2 Surface Coverage Model 18

2.2 Experimental 21

2.2.1 Materials 21

2.2.2 Surface Modification 23
2.2.2.1 Grignard Alkylation 23
2.2.2.2 Hydrogermylation 26
2.2.2.3 Thiolation 27
2.2.3 Elemental Surface Chemical Analysis 27
2.2.3.1 Instrumentation 27
2.2.3.2 Analysis 27
2.3 Results 30
2.3.1 Inorganic Modification 30
2.3.2 Alkylation 41
2.3.2.1 Methyl-Terminated Surfaces 41
2.3.2.2 Decyl-Terminated Surfaces 44
2.4 Discussion 47
2.4.1 Inorganic Surface Groups 47
2.4.2 Alkyl Groups 48
2.4.2.1 Methyl 48
2.4.2.2 Decyl 49
2.5 Conclusion 50

3 Electrical Measurements I: Surface Conductance 57

3.1 Introduction 57
3.1.1 Surface Recombination 58
3.1.1.1 Background 58

3.1.1.2 Photoconductivity Decay 61
3.1.2 Surface Charging 63
3.1.2.1 Surface Conductance 63
3.1.2.2 Pulsed Fields 65
3.2 Experimental 66
3.3 Results 69
3.3.1 Surface Conductance 69
3.3.2 Pulsed Fields 72
3.3.3 Silicon 73
3.4 Discussion 83
3.5 Conclusion 87

4 Electrical Measurements II: Mercury Contacts 92

4.1 Introduction 92
4.1.1 Background 92
4.1.2 Barrier Height Determination 94
4.1.3 Mercury Soft Contacts 96
4.2 Experimental 97
4.3 Results 98
4.4 Discussion 108
4.5 Conclusion 109

5 Transmission Infrared Absorption Spectroscopy 113

5.1 Introduction 113

5.1.1 Background 114

5.2 Experimental 119

5.3 Results 120

5.3.1 Methyl-Terminated Ge(111) Surfaces 120

5.3.2 Etched Surfaces 130

5.3.3 Decyl-Terminated Surfaces 136

5.4 Discussion 140

5.4.1 Methyl-Terminated Ge(111) Surfaces 140

5.4.2 Etched Surfaces 142

5.4.3 Decyl-Terminated Ge(111) Surfaces 144

5.5 Conclusion 144

A Python Script for Surface Conductance 149

List of Figures

1.1 Band-bending 4

1.2 Multijunction cell 9

2.1 Schemes for grafting alkyl monolayers to Ge(111) 15

2.2 XPS survey spectrum of clean Ge 17

2.3 Glassware: a. Extractor b. Modified drying chamber 24

2.4 Ge 3d region of HF-etched Ge(111) 30

2.5 Ge 2p region of HF-etched Ge(111) 31

2.6 Ge 3d region of HF-etched Ge(111) after one hour exposure to air . . . 31

2.7 Ge 2p region of HF-etched Ge(111) after one hour exposure to air . . . 32

2.8 Survey of Br-Ge(111) from HF-etched precursor 34

2.9 Ge 3d region of Br-Ge(111) from HF-etched precursor 34

2.10 Ge 2p region of Br-Ge(111) from HF-etched precursor 35

2.11 Br 3d region of Br-Ge(111) from HF-etched precursor 35

2.12 Survey of Br-Ge(111) from HCl-etched precursor 36

2.13 Ge 3d of Br-Ge(111) from HCl-etched precursor 36

2.14 Ge 2p of Br-Ge(111) from HCl-etched precursor 37

2.15 Br 3d region of Br-Ge(111) from HCl-etched precursor 37

2.16 Survey of CH_3S-Ge(111) 38

2.17 S 2p region of CH_3S-Ge(111) 39

2.18 Ge 3d region of CH_3S-Ge(111) 39

2.19 Ge 3d region of CH_3S-Ge(111) after 24 hours in air 40

2.20 S 2p region of CH_3S-Ge(111) after 24 hours in air 40

2.21 Survey of CH_3-Ge(111) 41

2.22 Ge 3d region of CH_3-Ge(111) 42

2.23 Ge 2p region of CH_3-Ge(111) 42

2.24 C 1s region of CH_3-Ge(111) 43

2.25 Survey of $C_{10}H_{21}$-Ge(111) prepared from Grignard reagent 44

2.26 Ge 3d region of $C_{10}H_{21}$-Ge(111) prepared from Grignard reagent 45

2.27 C 1s region of $C_{10}H_{21}$-Ge(111) prepared from Grignard reagent 45

2.28 Ge 2p region of $C_{10}H_{21}$-Ge(111) prepared from 1-decene 46

2.29 Ge 3d region of $C_{10}H_{21}$-Ge(111) prepared from 1-decene 46

3.1 Surface conductance vs surface potential 67

3.2 Conductance curves for the Ge (a) and Si (b) substrates used. The solid line is the more heavily doped of the pair. 70

3.3 Experimental setup 71

3.4 Conductance waveform of CH_3-Ge(111) surface in response to positive gate bias 75

3.5 Conductance waveform of CH_3-Ge(111) surface in response to negative gate bias 76

3.6 Conductance waveform of GeO_x-Ge(111) surface in response to positive gate bias 77

3.7 Conductance waveform of GeO_x-Ge(111) surface in response to negative gate bias 78

3.8 Negative gate bias applied to CH_3-Si(111) ($N_D=4 \times 10^{11}cm^{-3}$) 79

3.9 Negative gate bias applied to SiO_x-Si(111) ($N_D=4 \times 10^{11}cm^{-3}$) 80

3.10 Negative gate bias applied to CH_3-Si(111) ($N_D=7 \times 10^{13}cm^{-3}$) 81

3.11 Negative gate bias applied to SiO_x-Si(111) ($N_D=7 \times 10^{13}cm^{-3}$) 82

3.12 Surface recombination vs surface potential 84

4.1 Equivalent circuit 98

4.2 Representative *J*-*V* curves of alkylated Ge(111)/Hg Schottky contacts. Solid line is for n-type Ge(111) surface derived from decylmagnesium bromide, dashed line is undoped Ge(111) surface derived from methylmagnesium bromide, dotted line is from n-type Ge(111) derived from 1-decene. 101

4.3 Hg/$C_{10}H_{21}$-Ge(111) junction (wafer **III**) 102

4.4 Hg/CH_3-Ge(111) junction (wafer **III**) 103

4.5 Mott-Schottky plots for Hg/CH_3- and $C_{10}H_{21}$-Ge(111) junction (wafer **III**) 104

4.6 Hg/$C_{10}H_{21}$-Ge(111) junctions (wafer **I**) 105

4.7 Hg/CH_3-Ge(111) junctions (wafer **I**) 106

4.8 Mott-Schottky plots for Hg/CH_3-Ge(111) junction (wafer **I**) 107

5.1 Methyl group oriented normal to the Ge(111) surface 114

5.2 IR beam and sample wafer geometry for TIRAS 117

5.3 Beam and polarization geometry of IR radiation encountering dielectric surface 118

5.4 CD_3-Ge(111) vs CH_3-Ge(111) 121

5.5 External reflectance spectra of CH_3-Si(111) and CH_3-Ge(111) 123

5.6 CH_3-Ge(111) derived from surfaces etched with 6.0 M HCl or HBr, but not exposed to Br_2 vapor 125

5.7 CH_3-Ge(111) derived from surfaces etched with 6.0 M HCl then exposed to Br_2 vapor 126

5.8 CH_3-Ge(111) derived from surfaces etched with NH_4Cl-HF mixture then exposed to Br_2 vapor 127

5.9 CD_3-Si(111) and CD_3-Ge(111) 128

5.10 6.0 M HF(aq)-etched Ge(111) at 74° incidence 133

5.11 12.0 M HF(aq)-etched Ge(111) at 74° incidence 134

5.12 Effect of hydrocarbon in 6.0 M HF etchant 135

5.13 ν(C-H) region of $C_{10}H_{21}$-Ge(111) at 30° incidence 137

5.14 ν(C-H) region of $C_{10}H_{21}$-Ge(111) at 74° incidence 138

List of Tables

2.1 Procedures of Etching Ge(111) 25

2.2 XPS Analysis Parameters 29

2.3 Hydrocarbon Coverages 29

3.1 Equilibrium Surface Potential and Maximum SRV 84

4.1 Junction Properties of Hg/Ge(111) 100

5.1 Methylation Procedures 129

5.2 Position and Full-Width at Half-Maximum[a] of Alkyl Monolayer Infrared Absorption Modes 139

Chapter 1

Introduction

1.1 Background

1.1.1 Semiconductors

Ever since the development of crystal rectifiers for radar receivers in World War II, semiconductors have played an important role for over half a century in the form of electronics, and are expected to play a critical role in solar power generation.[1,2] Semiconductor theory and technology were established with crystalline semiconductors such as silicon (Si) and germanium (Ge), the latter of which is the focus of this work.

The band structure described in the following sections is a result of electrons moving within a periodic potential, such as that induced by the crystal lattice.[3] The periodicity of the bulk crystal cannot continue out past the physical surface, so there is necessarily a distortion of the crystal potential. Because the surface of the crystal is accessible to contact with other materials, the chemical composition at the surface may be quite different from that of the bulk. For this reason, knowledge and control

of the electronics and chemistry of the crystal surface is important for practical use of semiconductor devices.

1.1.2 Surface Potential

When a semiconductor is contacted with a conducting phase, there will be a net transfer of charge until the electrochemical potential of the materials are balanced by the electric potential of the field established at the interface. The conducting phase has a higher density of states than does the semiconductor within the bandgap, so while the charge on the conducting side is located at the interface, the charge in the semiconductor is distributed across a space charge region beneath the surface. The charge density of this region, and hence the width, is determined by the dopant concentration. For a uniform dopant density, it can be approximated that the dopant atoms are uniformly ionized and the carriers depleted to a certain depth. In the case of an n-type semiconductor brought into contact with a metal of lower chemical potential (higher work function), there will be a transfer of electrons to the metal so the metal surface has a negative charge, balanced by the positively charged immobile donor atoms in the semiconductor. This is depicted in Figure 1.1 on page 4. As a conduction band electron is brought to the interface, it is at a greater potential as it approaches the increasingly less-shielded negative charge on the metal. This is described by an approximation in Poisson's equation

$$\frac{\delta^2 V}{\delta x^2} = \frac{\delta E}{\delta x} \approx \frac{q}{\varepsilon_s} N_D \tag{1.1}$$

Integrating and eliminating E yields the relationship between the depletion width W, the dopant density N_D, and the difference in potential between the two phases or built in potential V_{bi}

$$W = \sqrt{\frac{2\varepsilon_s V_{bi}}{qN_D}} \tag{1.2}$$

The current-voltage behavior of the rectifier is dependent upon the concentration of carriers at the surface and available to cross the interface. That surface concentration differs from that of the bulk in a manner governed by the the built-in voltage

$$n_s = n_b \exp\left(\frac{-q(V_{bi} + V)}{kT}\right) \tag{1.3}$$

$$n_b = n_i \exp\left(-\frac{E_F + E_i}{kT}\right) \tag{1.4}$$

where n_s is the surface electron concentration, and n_b is the bulk electron concentration.

The simple model outlined above is complicated by the presence of surface-states. Electrically active surface-states alter the surface carrier concentrations, and the surface potential, by acting as carrier recombination or generation centers. The V_{bi} of a junction is also altered as the surface states accept or donate charge during the initial equilibration. These effects of surface-states are often uncontrolled and undesirable, and the chemical identity of the surface-states is dependent upon the semiconductor material type. For this reason, chemical control of the surface is of critical importance.

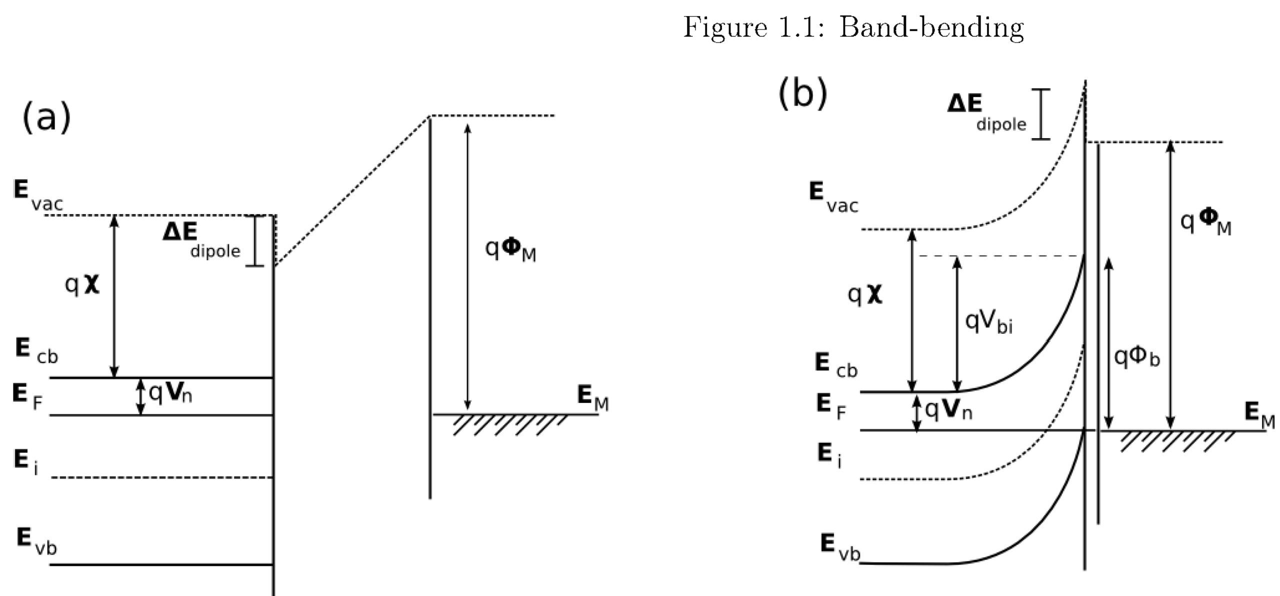

Figure 1.1: Band-bending

1.2 Silicon & Germanium

Covalent diamond-type semiconductors silicon and germanium are composed of a single element and may be melted and crystallized with a method first discovered by Czochralski for purifying metals.[4,5] For this reason, high purity crystals have long been produced to a degree not easily achievable with compound semiconductors.[6]

Although both Ge and Si have a diamond type crystal structure, reconstructed Si(111) and Ge(111) surfaces prepared in ultra-high vacuum (UHV) have different periodicity of surface atoms, resulting in different chemistries under such conditions. The bare Si(111) surface reconstructs to a 7×7 unit cell.[7] Under vacuum, bare Ge(111) tends to reconstruct to a c(2×8), with two distinct surface atom types, adatoms and restatoms. Adatoms bond to three atoms of the first full atomic layer, occupying 3/4 of the surface bonds of that layer. The restatoms are the remaining 1/4 of the full layer atoms that do not bond to the adatoms.[8,9] As confirmed by STM, charge transfer from the adatoms to the restatoms leads to filled and empty dangling bond types.[9,10] Chemically passivated surfaces on both Si(111) and Ge(111), however, display the 1×1 unit cell. The Ge lattice constant is approximately 4% larger than that of Si, so the distance between neighboring atop atoms of the (111) 1×1 surface is similar for both semiconductors (3.8 Å for Si(111) and 4.0 Å for Ge(111)) so that the two surfaces are geometrically comparable.[11,12]

In the 1950s, Ge and Si were both major components of the developing solid-state electronics field. With the advent of the field effect transistor, however, Si became the dominant material, though Ge has continued to be used in special components for

microwave and infrared communications. Silicon oxide is a stable material that may be grown on the crystal surface to form a gate dielectric. Under proper conditions, the crystal/oxide interface can be formed with a minimal electronic defect density.[13] Germanium oxide is water soluble and not stable under most relevant conditions, so that even if a low-defect crystal/oxide interface were to be formed it could not be maintained. For this reason, Si has been useful for technologies using field effect devices while germanium has been largely overshadowed.

In addition to electronics, Si is a dominant material in photovoltaics (PV). The use of crystalline Si for this purpose is in part due to the fact that there existed Si processing capabilities and technology developed for electronics. However, Si has other aspects that ensure that it will be an attractive PV material, even as the PV and electronics technologies diverge and world-wide PV module production outstrips the production of other electronic components. As a practical matter, Si is both non-toxic and abundant, so there is no inherent danger in its widespread use.[14]

1.2.1 Germanium

Electronics

There has been recent interest in Ge for use in field effect transistors. As the number of transistors on an integrated circuit increases, and the power per transistor must necessarily decrease, the gate oxide has decreased to less than 1 nm, and due to both electron tunneling and physical defects in such a thin layer, leakage currents become significant. In order to use a sufficiently thick dielectric that the leakage

currents are avoided without sacrificing the electrical performance of the transistor, silicon oxide is replaced with a high-κ material such as hafnium oxide.[13] With the removal of its oxide from the device architecture, Si no longer has this major advantage over Ge.

Ge possesses a hole carrier mobility that is four times that of the hole carrier mobility in Si, an advantage in high-speed circuits and of interest in CMOS technology where the p-channel component has traditionally had poorer performance.[13,15,16] Although the processing of Ge is similar to Si, it can take place at lower temperatures. Ge has a melting point of 937°C versus 1414°C for Si.

Light Absorption

A semiconductor will absorb incident radiation at or above the energy of its bandgap. Photon energy in excess of the bandgap is usually lost as heat. Silicon's 1.12 eV bandgap is also reasonably close to the 1.4 eV gap that would be ideal for efficient collection of sunlight, as represented by the AM 1.5 solar spectrum.[17,18] If the bandgap were larger, much of the incident light would not be absorbed. If the gap were smaller, more would be absorbed but more of the energy wasted as heat rather than producing a voltage. At 0.67 eV, the bandgap of Ge is much too small to efficiently capture solar radiation for useful electricity. However, it can be a component in multijunction solar cells, depicted in Figure 1.2 on page 9, where the higher energy photons are first collected by a wide bandgap absorber. The remaining lower energy photons are collected by a second or third absorber. Multijunction cells are more complicated, and hence more expensive, than single absorber cells. But the

similarity in processing to that of Si, and the similarity in lattice parameters to GaAs (1.6 eV gap) indicate that the choice of Ge could mitigate some of the complexity.[3]

1.3 Summary

Ge has much to offer in the fields of electronics and photovoltaics and has enough similarities to Si that comparable passivation techniques may be applied. The research described herein concerns an attempt to passivate the defects through a wet chemical technique similar to that proven to be successful in passivating Si. Elemental analysis of the modified surfaces is performed with x-ray photoelectron Spectroscopy (XPS). Structural analysis is performed with transmission infrared absorption spectroscopy (IRAS). Surface electronics are measured with combined surface recombination velocity (SRV) and low-frequency step-modulated field effect surface conductance measurements. Surface energetics are measured with n-Ge/Hg rectifying soft contacts.

Figure 1.2: Multijunction cell

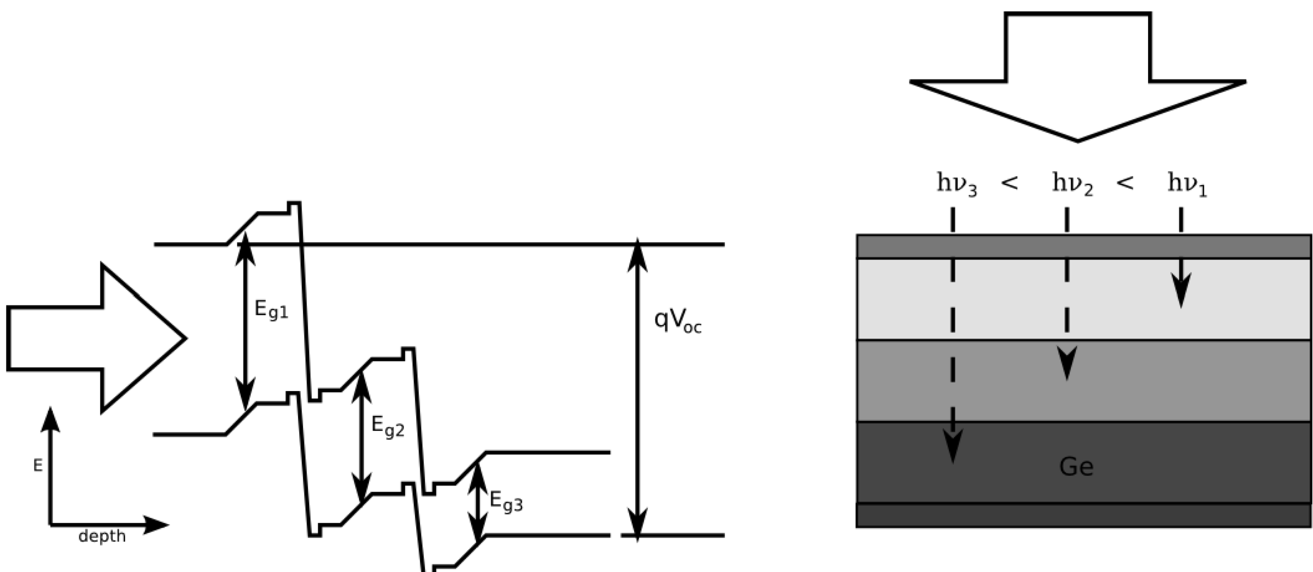

Bibliography

[1] Torrey, H.; Whitmer, C. *Crystal Rectifiers*; McGraw-Hill: New York, 1948.

[2] Riordan, M.; Hoddeson, L.; Herring, C. *Rev. Mod. Phys.* **1999**, *71*, S336–S345.

[3] Pierret, R. *Advanced Semiconductor Fundamentals*; Addison-Wesley Publishing Co.: Reading, Mass., 1989; Vol. 6.

[4] Wagner, R.; Chalmers, B. *J. Appl. Phys.* **1960**, *37*, 581–597.

[5] McCarty, L. *J. Electrochem. Soc.* **1959**, *106*, 1036–1042.

[6] Teal, G.; Little, J. *Phys. Rev.* **1950**, *78*, 647.

[7] Duke, C. *Chem. Rev.* **1996**, *96*, 1237–1259.

[8] Chadi, D.; Chiang, C. *Phys. Rev. B* **1981**, *23*, 1843–1846.

[9] Razado-Colambo, I.; He, J.; Zhang, H.; Hansson, G.; Uhrberg, R. *Phys. Rev. B* **2009**, *79*, 205410.

[10] Becker, R.; Swartzentruber, B.; Vickers, J.; Klitsner, T. *Phys. Rev. B* **1989**, *39*, 1633–1647.

[11] Yu, H.; Webb, L.; Solares, S.; Cao, P.; Goddard, W.; Heath, J.; Lewis, N. *J. Phys. Chem. B* **2006**, *110*, 23898–23903.

[12] Cao, S.; Tang, J.-C.; Shen, S. *J. Phys.: Condens. Matter.* **2003**, *15*, 5261–5268.

[13] Houssa, M.; Chagarov, E.; Kummel, A. *MRS Bull.* **2009**, *34*, 504.

[14] Haxel, G.; Hedrick, J.; Orris, G. *Fact Sheet 087-02 Rare Earth Elements — Critical Resources for High Technology*, http://pubs.usgs.gov/fs/2002/fs087-02/.

[15] Frank, M. M.; Koester, S. J.; Copel, M.; Ott, J. A.; Paruchuri, V. K.; Shang, H.; Loesing, R. *Appl. Phys. Lett.* **2006**, *89*, 112905.

[16] Brunco, D. et al. *J. Electrochem. Soc.* **2008**, *155*, H552–H561.

[17] Shockley, W.; Queisser, H. *J. Appl. Phys.* **1961**, *32*, 510.

[18] Sze, S. *Physics of Semiconductor Devices*, 2nd ed.; John Wiley & Sons: New York, 1981.